Vol. 42, No. 4 (2020) 529-546, DOI: 10.24874/ti.870.04.20.09

Tribology in Industry

www.tribology.rs

RESEARCH

Friction and Wear Properties of Rapid Solidified H-Al-17Si Alloys Processed by UV Assisted Stir - Squeeze Casting with DLC-Star (CrN + a-c:H) Coating Under HFRR

N.D. Malleswararao. K[a,*], I.N. Niranjan Kumar[b], Bh. Nagesh[c]

[a]*Department of Marine Engineering, Andhra University, Visakhapatnam, A.P, India,*
[b]*Department of Marine Engineering, Andhra University, Visakhapatnam, A.P, India,*
[c]*Indian Maritime University, Visakhapatnam, Andhra Pradesh, India.*

Keywords:

Stir-squeeze casting
AlSi MMC
DLC-star coating
Friction
Wear

* Corresponding author:

N.D. Malleswararao. K
E-mail: nottymalli@gmail.com

Received: 7 April 2020
Revised: 22 May 2020
Accepted: 5 September 2020

A B S T R A C T

Tribological properties of rapid solidified hyper eutectic AlSi17Cu3.5-4Mg0.6-0.8 (H-Al-17Si) alloy were investigated under different loading conditions. The alloy was produced by the rheo-stir squeeze casting process with the T-6 condition. Experimental studies were conducted using high frequency linear reciprocating rig (HFRR) with a ball-on-plate geometry. The effect of applied load (10-50 N) on the wear and friction (COF) coefficients were studied under dry, lubricated (SAE15W40), and coated dry (DLC-Star) sliding conditions. For dry and lubricated sliding, COF values of hyper eutectic AlSi17Cu3.5-4Mg0.6-0.8 alloy were 0.26 and 0.042. A lower COF value of 0.013 was recorded with DLC-star (CrN + a-c:H) coating under dry condition. Whereas, the least wear coefficient is also observed with DLC-star coating (4.6X10^{-5} mm^3/N.m) compared to the dry and lubricated sliding conditions (2.7X10^{-3} mm^3/N.m and 3.8X10^{-4} mm^3/N.m). The developments in COF and wear coefficients were mainly attributed to the distribution and size of primary Si granules and the formation of transfer layers on the coated surfaces of AlSi17Cu3.5-4Mg0.6-0.8 alloy. Surface morphologies were examined using SEM, AFM, surface roughness profilometer, and advanced metallurgical microscope (AMM) analysis techniques.

1. INTRODUCTION

The performance of an automobile engine depends much on tribological properties and emission losses [1]. However, the tribology of a mechanical system is very difficult, being controlled by several factors, including lubricants, surface structure, contact geometry, speed, distance, and load [2]. Over the past few decades, researchers have developed numerous wear and friction solutions in terms of nano-lubricants, surface coatings, lightweight composites, for the manufacturing of high performance engine components to enhance efficiency, reduce emission, wear and friction losses [3-5].

In the last 20 years, hypereutectic Al-Si alloys (H-Al-Si MMCs) are promising materials to increase efficiency and reduce emissions [6,7]. H-Al-Si MMCs possess excellent thermal resistance, corrosion resistance, abrasion resistance, and high specific strength [8-10]. Whereas, the traditional cast H-Al-Si alloys reached their limits of resisting heat and elevated temperature strength as the engine power increased [11]. Thus the researchers developed new casting techniques including spray deposition, powder metallurgy, and planar flow casting on rapid solidification to prepare high strength and high heat resistant Al alloys [12,13]. However, these new techniques are challenging to execute, and the dimensions of the components are also limited [11]. The use of ultrasonic vibration during the stirring of Al-Si MMCs and squeeze is a comparatively new method [14]. It is a user-friendly technique with the benefits of low cost and simple operability [15-18]. Vineet Tirth et al. and Khemraj et al. explored the effect of stir-squeeze casting on the tribological properties of hybrid aluminum matrix composite. They reported that the stir-squeeze casting process substantially improved the hybrid composite [19-22]. H-Al-Si alloys are usually characterized as the composite where Si percentage is equal to or greater than 17 wt%. The addition of Si like hard particles enhances the hardness, which in turn improves the alloys (H-Al-Si) wear-resisting properties [23, 24]. Clarke et al. explored the wear behavior of Al-Si metal matrix composites (MMC = alloy) by changing Si weight percentage (up to 21 wt%) and stated that the hyper eutectic MMCs have low wear resistance than hypoeutectic MMCs [25]. However, Reddy et al. carry out some wear tests on a series of MMCs (AlSi) changing Si weight percentage up to 23 wt% and addressed that the reinforcement of hard primary Si particles to alloy matrix enhances wear resistance of H-Al-Si MMCs [26]. Thus the reinforcement of Si granules to the alloy matrix enhances both tribological and mechanical properties.

Numerous tribological studies reported on the wear and friction characteristics of Al-Si MMCs [27,28]. Though, over the past few years, one of the solutions for reducing wear and friction in automobile components is lubricant oils [29]. Dey et al. executed tribological studies on Al-Si (18.5 wt%) MMCs by varying load 0.5–5 N under the lubricated condition and found that few scratch marks are only left on the surface by Si particles, and alloy matrix was glued to the counterpart when the load increased [30]. Later, Parveen Kumar et al. investigated the tribological behavior of AlSi25 MMC with different loading conditions (5-100 N) under lubricated and dry conditions using an LRT (linear reciprocating tribometer). In this study, it was noticed that with lubricating oil (SAE20W40) remarkable reduction in COF and wear coefficient is achieved [31]. Further, the investigation continued by varying load 100-300 N and stated that at excessive loads, the MMC Si-particles were jutted out then mixes with lubricating oil and performs as a solid lubricant which results in substantial improvement in COF and wear rate [32]. However, these conventional lubricants cannot withstand the latest higher-powered engines for a long time at extreme loads and temperatures; the need for developing high-performance lubricating fluids is significantly increasing.

Scholars examined the tribological behaviors of nanoparticles as lubricant oil additives. It has been found that the reinforcement of nanoparticles into the lubricating oil improves the load-carrying capacity and reduces COF and wear rate [33-35]. However, at raised temperatures, large protuberances founded on the counterpart surfaces may increase wear and friction coefficients. To solve this problem, researchers tend to add fullerene (IF-Mos2 and h-BN) like nanoparticles into the lubricant liquids (SAE15W40), reported that the reinforcement of IF-Mos2 and h-BN nano granules into the lubricating oil enhances the anti-wear and friction properties remarkably [36-39]. From the above literature, it is observed that the reinforcement of nanoparticles into the lubricating oil improves the COF and wear performance of automobile components.

Though, the journey of finding a perfect lubricant, which gives the least tribological properties, still proceeds [40]. An energizing substance that has been examined broadly for its vast number of tribological and mechanical characteristics is Diamond-like carbon (DLC). In general, these coatings (DLC) show excellent corrosion resistance, higher hardness, high thermal stability, and extreme tribological properties. However, the friction and wear properties heavily influenced by temperature and humidity [41-47]. Moreover, some studies show that the hydrogenated-amorphous DLC layers (a-C:H) are the promising wear and COF resistant coatings at different environmental conditions [48-50]. Erdemir et al. reported that the hydrogen plays an essential role in determining the tribological characteristics of DLC coatings due to preventing graphitization and formation of stabilized sp3 tetrahedral bonds. However, a-C:H coatings show excellent tribological properties for Al alloys at the ambient conditions compared to the other coatings like CrN and TiN [51-56]. Besides, few scholars investigated the performance of DLC coatings on Al-alloys with inert gas and dry nitrogen environmental conditions and reported that the reduction in friction coefficient (0.001-003) is remarkable, and the wear rate (10^{-10}–10^{-11} mm3/Nm) was improved mainly [44,45,57]. Later, researchers conducted several experiments on a-C:H films at elevated temperatures and reported that the COF decreases, and the wear scars become deeper, bigger, and softer [58-69]. From these studies, it is clear that the DLC coating has extraordinary potential as a hard film to combat COF and wear rate in different tribological uses.

It is evident from the above studies that the tribological characteristics of Al-Si MMCs depend on manufacturing routes [73] and the Si content [7,23,24,70-74]. Besides, the tests such as lubrication oils, nano lubricants, and DLC coatings also much influence the wear and friction coefficients of the MMCs.

The present research aims at the effect of the casting process and coatings on tribological properties of hypereutectic aluminum-silicon alloys, which are popularly used in the automotive industry. However, the use of DLC-Star coating with RSSC Al-Si alloy has not been reported in published research. It is desirable to apply the coating on Al-Si alloys for better friction and wear properties. The metal matrix composites (alloys) recognized for this research are Al17Si3.5-4Cu0.6-0.8Mg, one of the widely used alloys in the automobile industry. The alloys have good potential for higher temperatures, hardness, and wear applications in production and automobile industries. However, the coatings identified for this study have been deposited by a combined PVD/PACVD method, which has been selected based on the literature review.

2. EXPERIMENTAL DETAILS

2.1 Materials and specimens preparation

The hyper eutectic AlSi17Cu3.5-4Mg0.6-0.8 (H-Al-17Si) alloy was prepared by using rheo stir-squeeze (rheo = ultrasonic vibration (UV) assisted) casting technique under T-6 condition (RSSC-T6). However, the H-Al-17Si alloy (Table 1) was processed with stir casting with UV treatment primarily and then carries on by squeeze casting procedure. The schematic diagram (Fig. 1) mainly consists of a furnace with stir casting setup, squeeze casting setup, UV generator, and titanium alloy horn. The used frequency for this UV test was 20 kHz, and the highest power output was 2.8 kW.

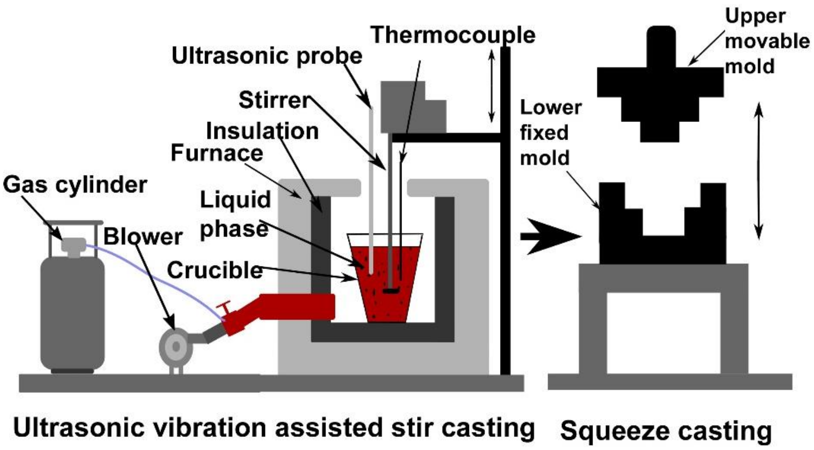

Fig. 1. Rheo stir-squeeze casting process.

Table 1. Chemical composition of Al-17Si alloy.

Alloy	Fabrication Technique	Chemical Composition (wt%)			
		Si	Cu	Mg	Al
AlSi17	Rheo stir squeeze casting (RSSC)	17	3.5-4	0.6-0.8	Balance

The process begins with the melting of materials like pure Al and Cu in a gas furnace at 1100 °C. When the composite was completely liquified, then it was cooled to 720 °C and stirred mechanically. Preheated silicon and magnesium (270 °C) granules were added into the stir vortex by keeping the speed of 300 rpm around 15 min. The compound was again heated to 650 °C, and UV was applied for about 5min. After mixing with UV completed, the alloy was poured into a steel mold, which is already heated at a temperature of 200 °C. A pressure of 200 MPa was applied in both directions (up and down) with a holding time of the 60 s. Then the rapidly solidified square casting billet with 40x40x100 mm was achieved (Fig. 2). Figure 3 reveals the microstructure and chemical combination of H-Al-17Si alloy, and the elements weight percentages were indicated in Table 2. Further, the alloy (H-Al-17Si) was undergone through the heat-treatment operation with the T-6 condition. The T-6 process consists of a solution heat treatment (500 °C) with a soaking time of 4 hours and then rapid quenching in water (<50 °C) later it was carried on with artificial aging at 165 °C for 4 hours and then cooled in air. Square specimens of 40x40x10 mm were sliced out (Fig. 4) from the heat-treated billet. Whereas to understand the mechanical properties (Tables 3 and 4) of H-Al-17Si alloys, the hardness (ASTM E10-15) (Fig. 5) and tensile properties (ASTM E8 / E8M) (Fig. 6) were investigated using Brinell hardness equipment and Tensometer.

Table 2. EDS analysis of Al-17Si alloy.

S.no	Alloy	Elements (wt%)					
		Si	Cu	O	Mg	C	Al
1	AlSi17	15.98	3.61	1.12	0.47	4.99	73.83

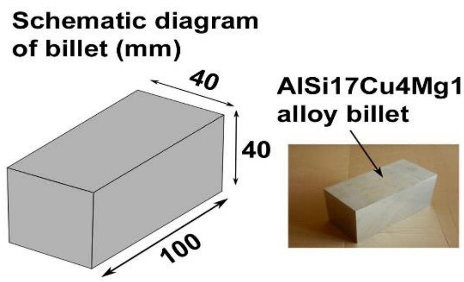

Fig. 2. H-Al-17Si alloy billet.

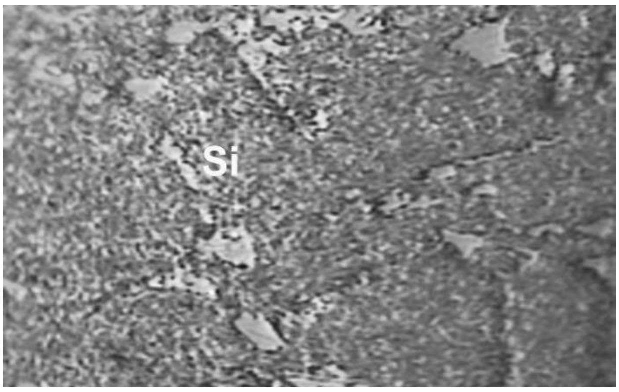

(a)

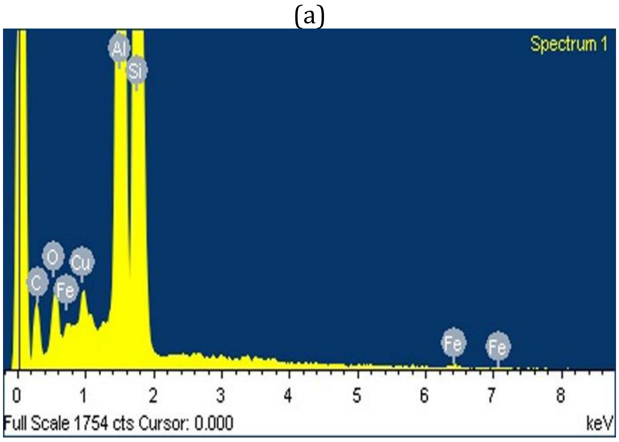

(b)

Fig. 3. (a) AlSi17Cu3.5Mg0.8 alloy Microstructure; (b) AlSi17Cu3.5Mg0.8 alloy EDS analysis.

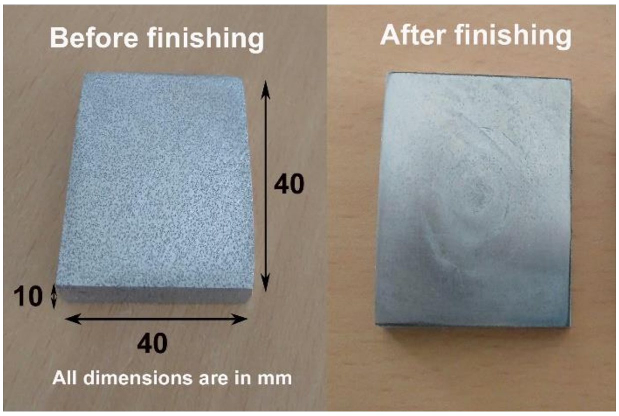

Fig. 4. H-Al-17Si alloy samples before and after finishing.

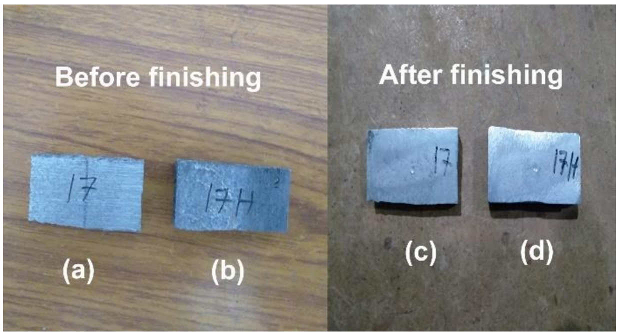

Fig. 5. Hardness test samples (a and c) before heat treated, (b and d) after heat treated.

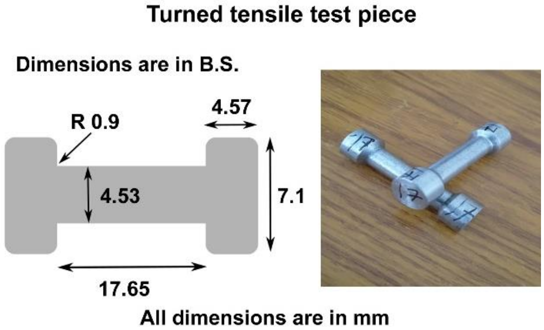

Fig. 6. Tensile test samples.

Table 3. Hardness values of Al-Si alloys.

Composition	Load (kgf)	Ball diameter (mm)	Hardness value before heat treatment (BHN)	Hardness value after heat treatment (BHN)
AlSi17	250	5	106.82	179.37

Table 4. Tensile properties of Al-Si alloys.

Composition	UTS		YS		Elongation (%)	
	RSSC	RSSC-T6	RSSC	RSSC-T6	RSSC	RSSC-T6
AlSi17	261	386	235	312	2.1	0.8

2.2 DLC-Star coating

Oerlikon Balzers supplied the metal-free amorphous carbon (CrN+a-c: H) coating (Table 5) used in this investigation. They were deposited by a combined PVD/PACVD method on a square plate of H-Al-17Si alloy with a thickness of 4 µm. The coated surface was polished during the finishing process to remove the extra particles, and droplets maybe adhere to the top of the specimens (Fig. 7).

Table 5. Properties of DLC-Star coating.

Coating properties	Value
Coating material	CrN + a-C:H
Typical microhardness (HK 0.01)	>2000
Typical coating thickness (µm)	2 - 4
Coating temperature (⁰C) Maximum service temperature (⁰C) Coating color	<250 350 Black

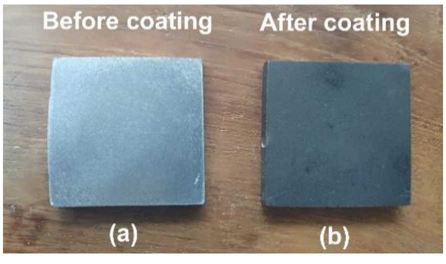

Fig. 7. H-Al-17Si samples (a) before coating, (b) after coating.

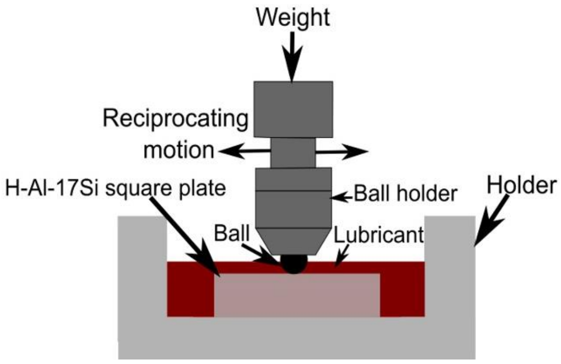

Fig. 8. HFRR setup.

2.3 Tribological tests description

Friction and wear experiments were conducted at room temperature using HFRR (High frequency linear reciprocating rig – ASTM G133) (Fig. 8) with a ball (10mm diameter) on a plate (square) geometry under dry, coated and lubricated conditions. All lubricated experiments are carried out with engine oil synthetic grade SAE15W40 as a lubricant (Table 6). The uncoated H-Al-17Si specimens (40x40x10 mm) surface preparation is done by polishing with Si-C papers (1000 and 800 grit size), and the final mirror finishing is achieved with diamond paste (1 µm). After polishing, the specimens are cleaned with benzene and acetone to remove any detritus that may have been left during finishing (Fig. 4). The applied load range during the friction and wear test was 10-50 N at a 20 Hz frequency. The reciprocating experiment time was 10 min with a stroke length of 2 mm and a sliding distance of 50 m. AMM (VFM-9100 Metzer Meta vision), AFM surface roughness profilometer (Veeco), and SEM (S-3700N) were used to study the microstructures of the alloys. After that, the friction coefficient values are directly obtained by the HFRR screen, and the wear coefficient (Kw) of the alloys was calculated using the following equation (1).

$$\text{Wear coefficient} = \frac{\text{Wear volume}}{\text{(Applied Load X Sliding diatance)}} \quad \frac{mm^3}{N.m} \qquad (1)$$

where wear volume is denoted as W_v (mm³), sliding distance is denoted as S_d (m), and the applied load is denoted as F_n (N).

Table 6. Properties of lubricant oil grade SAE15W40.

Lubricant properties	Value
Kinematic viscosity @100°C, cSt	14.0-15.2
Viscosity index	130
Flash point	220°C
Pour point	-21°C

3. RESULTS AND DISCUSSION

The investigation contains three types of tests:

(1) H-Al-17Si MMC against AISI52100 ball in dry condition.

(2) H-Al-17Si MMC against AISI52100 ball in lubricated (SAE15W40) condition.

(3) H-Al-17Si MMC against AISI52100 ball in coated (DLC-Star) dry condition.

3.1 Coefficient of friction (COF)

Figure 9 shows the friction (mean value and standard deviation) values obtained from the experiments.

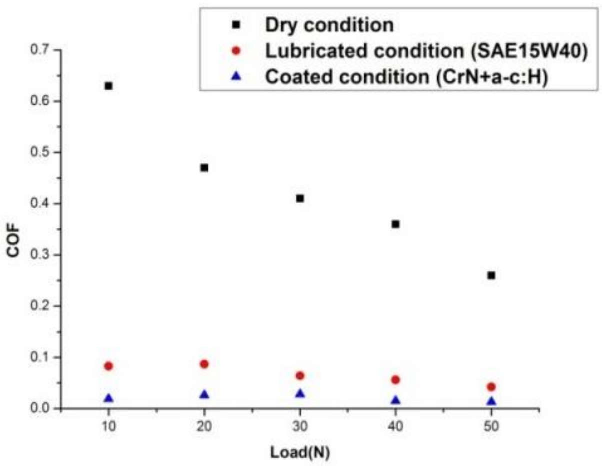

Fig. 9. COF (mean value and standard deviation) versus applied load for H-Al-17SI alloy.

However, they were plotted in graphs using standard deviation (0.20) values. The friction coefficient for H-Al-17Si MMC against AISI52100 ball in dry sliding condition was initially recorded a high value as 0.63 for few seconds then obtained a steady value of 0.26. However, a constant friction coefficient value of 0.042 and 0.013 was obtained in the case of SAE15W40 lubricating oil and DLC-Star coating. It is evident from the above results (Fig. 9) that the lowest friction coefficient value of 0.013 was achieved in the case of DLC-Star coating condition compared to dry (0.26) and lubricated (0.042) sliding conditions.

3.2 Wear coefficient

The wear coefficient is determined by the ratio of W_v (wear volume) of MMC plate per F_n (applied load), per S_d (sliding distance). However, wear volume is estimated using the weight loss method where the alloy disc weight is measured before and after the sliding tests using an electronic balance. The (K_w) wear coefficient (mean value and standard deviation) results procured for the H-Al-17Si MMC plate under dry, lubricated, and coated dry conditions are shown in Fig. 10.

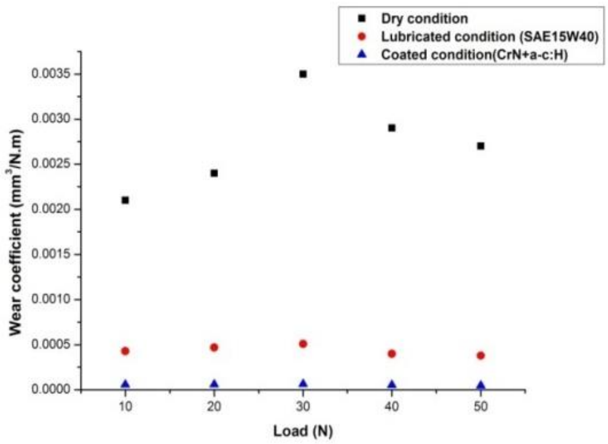

Fig. 10. Wear coefficient (mean value and standard deviation) versus applied load for H-Al-17Si alloy.

Whereas the wear coefficient graphs are plotted with mean and standard deviation (0.28) values. It can be observed that the highest wear coefficient value of $2.7X10^{-3}$ $mm^3/N.m$ was attained for H-Al-17Si MMC under dry condition. Whereas, wear coefficient values of $3.8X10^{-4}$ $mm^3/N.m$ and $4.6X10^{-5}$ $mm^3/N.m$ were acquired for the H-Al-17Si MMC plate when lubricated and coated dry conditions respectively. It is explicit from Fig. 10 that the highest wear coefficient value of 0.0027 $mm^3/N.m$ was attained under dry conditions, and the lowest wear coefficient of 0.000046 $mm^3/N.m$ was attained in case of coated (DLC-Star) dry conditions.

3.3 Analysis of friction

From Fig. 9, it is observed that the friction coefficient of the H-Al-17Si MMC plate against AISI52100 ball under dry state decreases (58.73 %) with increasing applied load (10 to 50 N). It is because of the presence of primary hard Si granules in the wear track of the H-Al-17Si MMC disc. Though, the Si granules distribution and size perform a significant role in the reduction of COF at increased applied loads. Initially, at 10 N applied load highest COF (Fig. 9) is recorded due to the high spots on H-Al-17Si disc surfaces that come into contact during sliding and stick to the AISI52100 ball surface which results in increased friction coefficient. Moreover, Fig. 9 shows that the friction coefficient decreases with the increased applied load (10-50 N). This reduction in COF mainly attributed to the formation of oxide-layers during sliding as the applied load increased. At higher applied loads, the hard Si granules jut out from the worn faces of H-Al-17Si MMC disc and act as ball bearings at the contact surfaces during sliding. In the case of SAE15W40 engine oil, the coefficient of friction remarkably decreased. From Fig. 9, it is seen that the friction coefficient is reduced from 0.083 to 0.042, which is nearly 49.4 % with the increase of applied load (10-50 N). This is because of the development of oil films between the tribopair. When the load increases, the COF decreases due to the hard Si particles of H-Al-17Si MMC mixes with lubricating oil and acts as a solid lubricant. The friction behavior of DLC-Star coated H-Al-17Si alloy is significantly improved compared to the lubricated (69.05 %) and dry (95 %) conditions. In the case of coated (DLC-Star) dry condition, the friction coefficient is significantly decreased (0.028-0.013) about 53.6 % with the increase in applied (10-50 N) load, as shown in Fig. 9. Such a reduction in friction coefficient due to the highly absorbed Si particle grain improvement and the development of tribo-oxidation films between the mating parts. It is clear from the above values (Fig. 9) that the friction coefficient of H-Al-17Si MMC is greatly affected by the highly absorbed Si granules [61] and the coated materials. Additionally, the fabrication process of H-Al-17Si MMC [62] also contributed to achieving a decreased coefficient of friction results. Unique characteristics of CrN + a-c:H (DLC-Star) coating on the surface of the alloy resulted in the lowest friction coefficient in H-Al-17Si MMC, which can strongly affect friction.

3.4 Analysis of Wear

From Fig. 10, it is noticed that the wear coefficient of the MMC increases (12.5 %) slowly with an increase in applied load (10 N to 30 N), but after 30 N (applied load) the wear coefficient instantly increases (31.43 %) and attains a steady-state value between 40-50 N loads. Whereas, in the case of lubrication with SAE15W40 oil and coated dry conditions the wear coefficient first increases about 15.7 % (10-30 N) and then again decreases about 11.5 % (30-50 N).

Optical and SEM images (Figs. 11-16) of the worn surfaces of dry conditions show deep scuffed tracks, stern abrasion, deep scratches, and stern surface plastic deformation due to the straight contact of the H-Al-17Si MMC disc with AISI52100 ball. Stern wear rate can be noticed on the H-Al-17Si MMC disc in dry condition without lubrication and coating. The SEM and optical images (Figs. 11-13) showed that the stern wear tracks have existed on the surface of the MMC, revealing that due to tribopair direct contact, high wear coefficient was recorded. Throughout the testing duration, wear coefficient enhanced linearly with the increase in applied load up to 30 N, as the load is more increased from 30-40 N the wear coefficient instantly increases about 17.14 % and attains a steady-state value at 40-50 N.

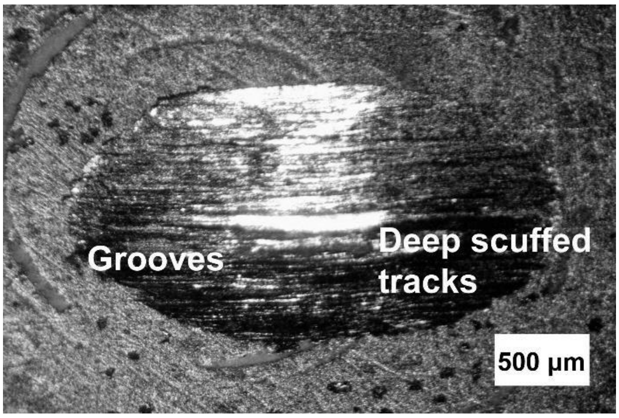

(a)

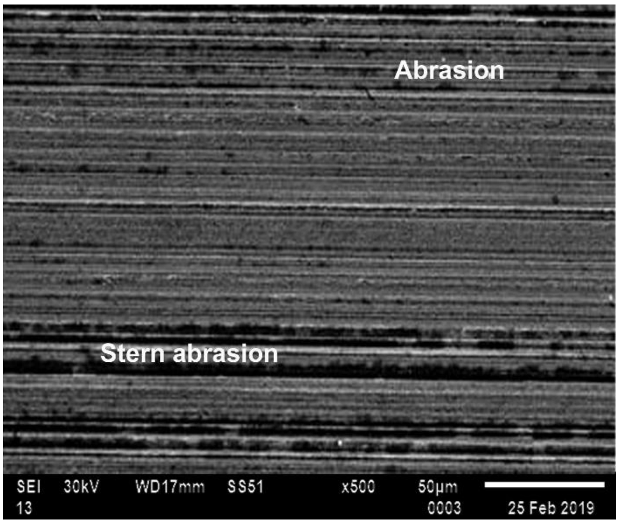

(b)

Fig. 11. (a) Optical micrograph of H-Al-17Si alloy at 10 N load under dry condition, (b) SEM micrograph of H-Al-17Si alloy 10 N load under dry condition.

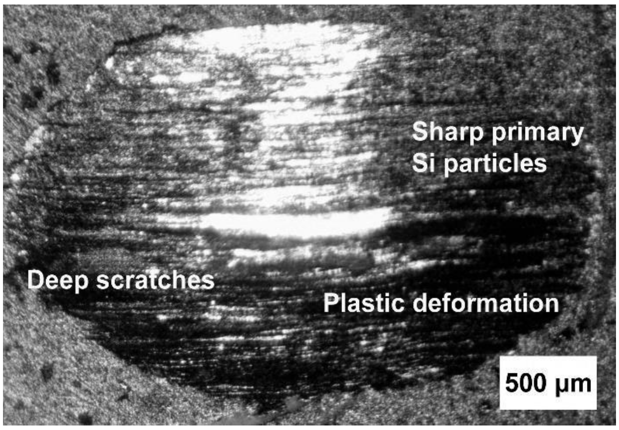

(a)

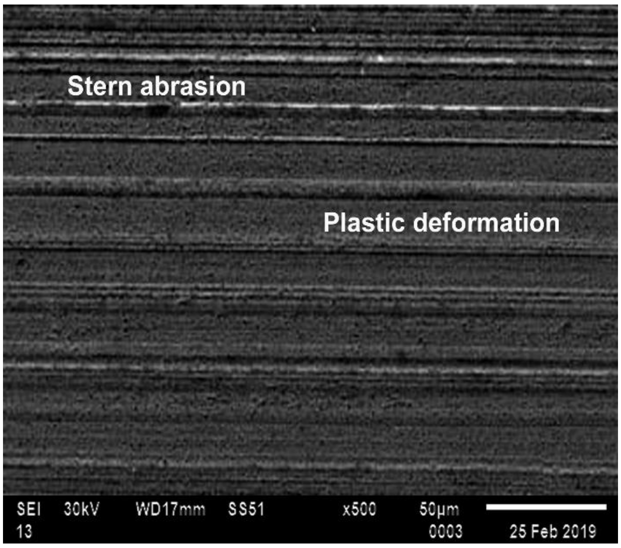

(b)

Fig. 12. (a) Optical micrograph of H-Al-17Si alloy at 40 N load under dry condition; (b) SEM micrograph of H-Al-17Si alloy 40 N load under dry condition.

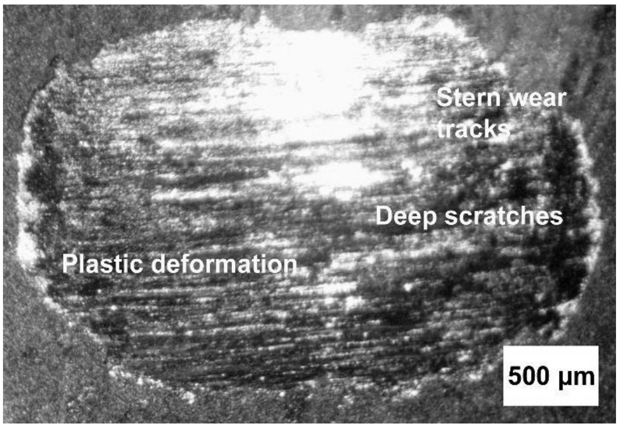

(a)

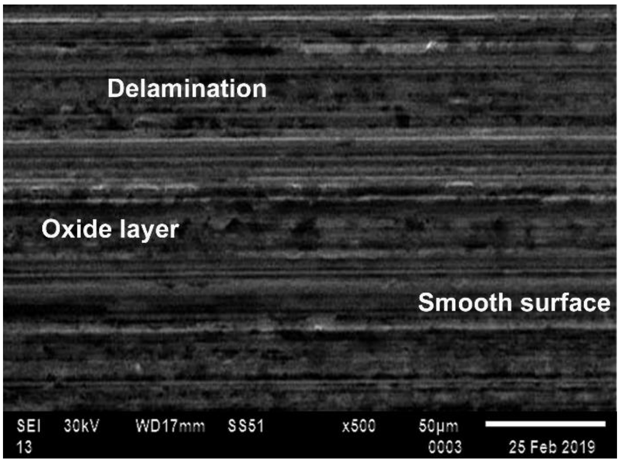

(b)

Fig. 13. (a) Optical micrograph of H-Al-17Si alloy at 50 N load under dry condition; (b) SEM micrograph of H-Al-17Si alloy 50 N load under dry condition.

Throughout the testing period, the contact between tribopair revealed at (asperity level) micro-level. During this level, both surfaces of tribopair rubbed subsequently, and the broken asperities (i.e., Al, Si, and Fe) transfer from H-Al-17Si disc to AISI52100 ball and ball surface to alloy disc, respectively. This leads to adhesion and also the mutual transfer of materials between disc and ball surfaces. Optical micrographs (Fig. 11 & 14) of H-Al-17Si MMC disc and AISI52100 ball confirm the abrasion occurred due to the protruded primary silicon particles get entrapped between the mating surfaces. From Figs. 12 & 15, it is explicit that when the load increases, the abrasion level decreases due to the primary Si particles get distorted and a formed thin oxide layer.

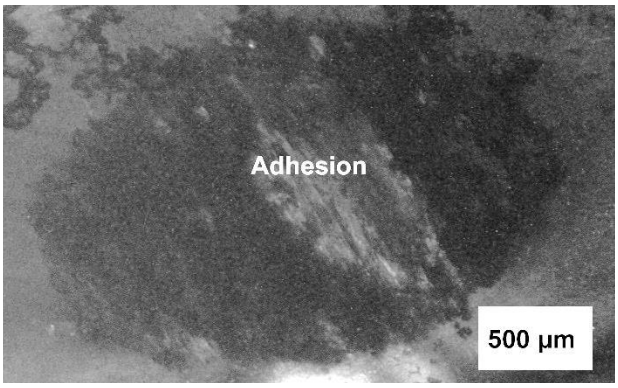

(a)

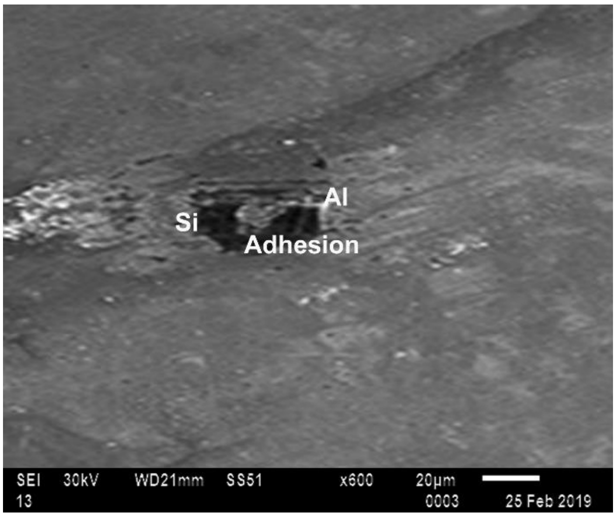

(b)

Fig. 14. (a) Optical micrograph of steel ball at 10 N load under dry condition; (b) SEM micrograph of steel ball at 10 N load under dry condition.

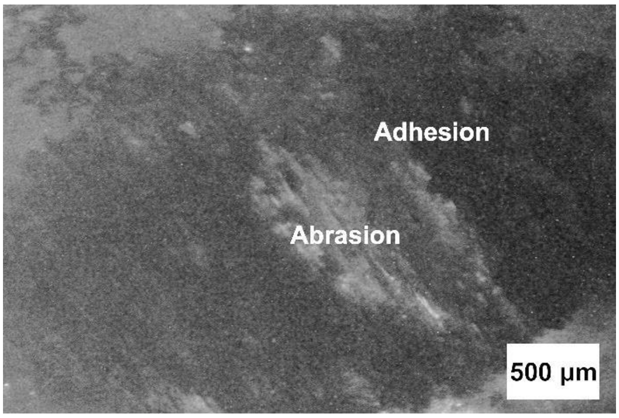

(a)

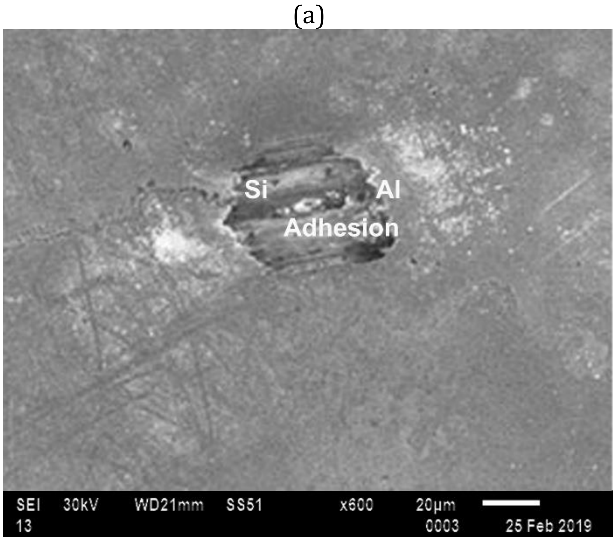

(b)

Fig. 15. (a) Optical micrograph of steel ball at 40 N load under dry condition; (b) SEM micrograph of steel ball at 40 N load under dry condition.

The formed oxide layer acts as a solid lubricant between mating surfaces at higher loads (30 N-50 N) and reduces the wear coefficient. Whereas, optical and SEM images (Figs. 13 & 16) confirm the development of the oxide layer and the existence of distorted Si granules on the wear tracks. From the above, it is clear that adhesion, abrasion, thin oxide layer developments were the superior wear mechanism under dry conditions.

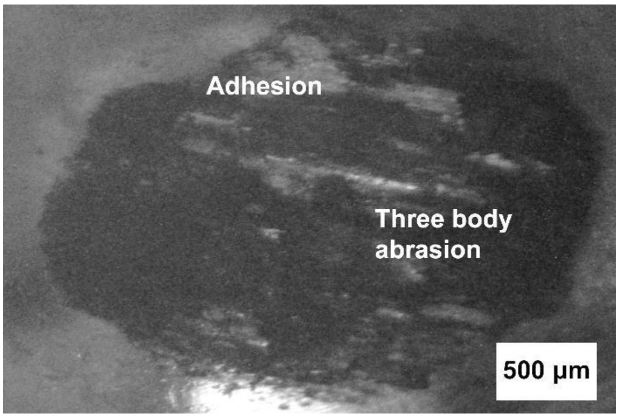

(a)

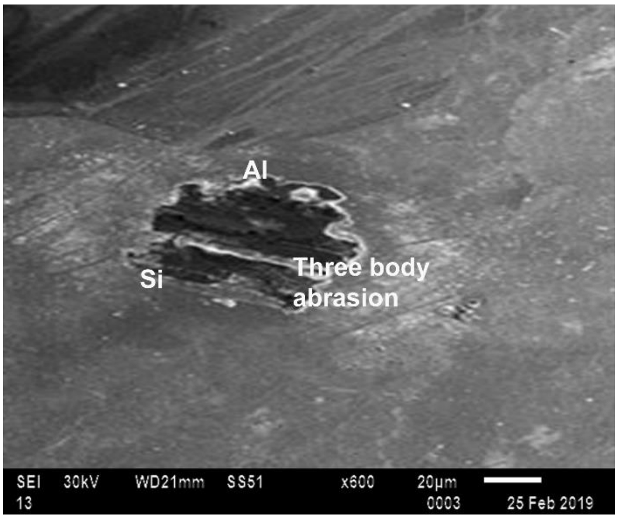

(b)

Fig. 16. (a) Optical micrograph of steel ball at 50 N load under dry condition; (b) SEM micrograph of steel ball at 50 N load under dry condition.

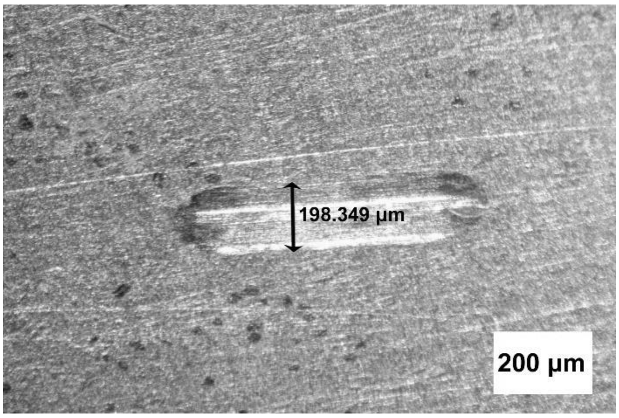

(a)

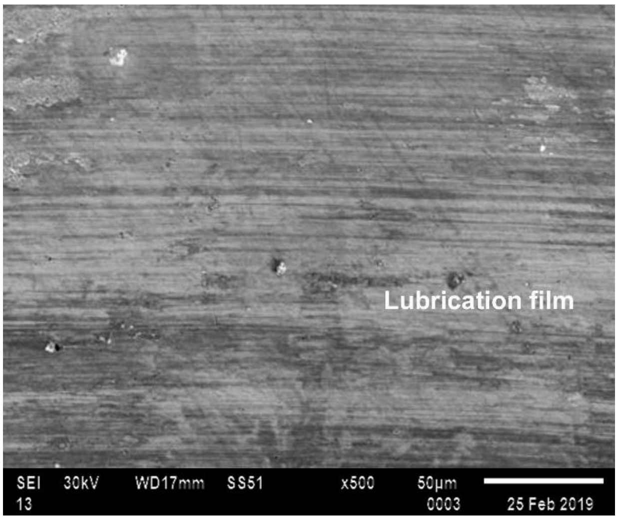

(b)

Fig. 17. (a) Optical micrograph of H-Al-17Si alloy at 30 N load under lubricated condition; (b) SEM micrograph of H-Al-17Si alloy at 30 N load under lubricated condition.

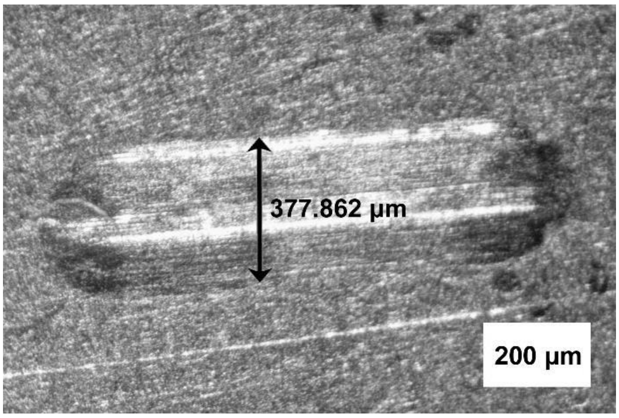

(a)

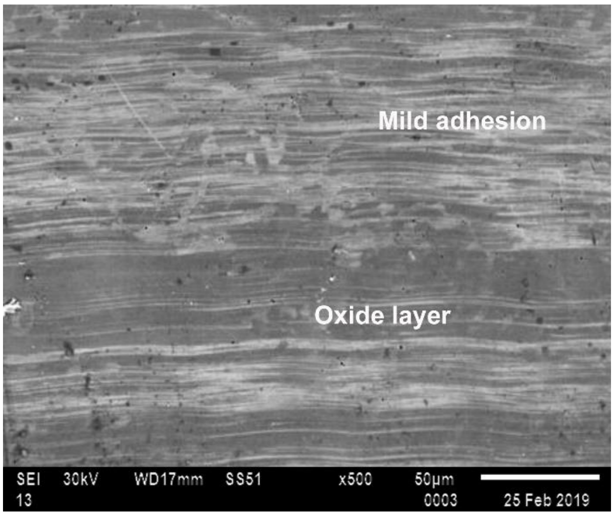

(b)

Fig. 18. (a) Optical micrograph of H-Al-17Si alloy at 50 N load under lubricated condition; (b) SEM micrograph of H-Al-17Si alloy at 50 N load under lubricated condition.

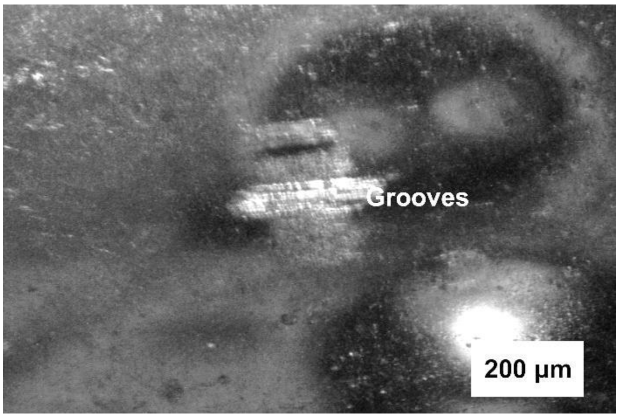

(a)

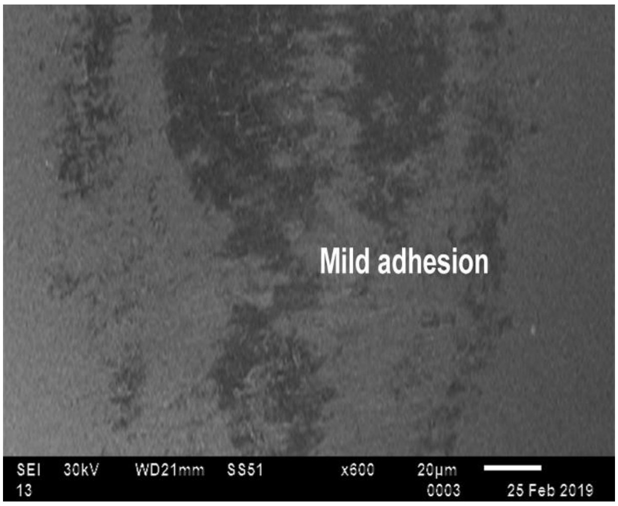

(b)

Fig. 19. (a) Optical micrograph of steel ball at 30 N load under lubricated condition; (b) SEM micrograph of steel ball at 30 N load under lubricated condition

In the case of lubrication with SAE15W40 oil, the wear coefficient was reduced extremely (about 86 % compared to dry) (Fig. 10). This is because of the development of oil film between tribopair, which avoids straight contact between mating surfaces. The formed oil film between H-Al-17Si MMC disc and AISI52100 ball reduces abrasion, adhesion, and plastic deformation remarkably, which decreases the in wear coefficient significantly. At lower (10 N) applied load, the wear tracks are very less, and fewer grooves with dense wear scars are present on the alloy surface. Whereas, at 30 N applied load, Fig. 17 &19 shows light adhesion of asperities, which will marginally increase the wear coefficient of the H-Al-17Si disc. Further, profilometer images also clearly show the increased wear scars with an obtained roughness value of 3.20 µm (Fig. 26a) as compared to the roughness value of 0.104 µm at an applied load of 10 N. At 50 N applied to load the wear coefficient (1.35 µm)

(Fig. 26b) again decreases compared to the 30 N applied load. This is due to Si granules mix with SAE15W40 lubricating oil and acts as solid lubricant and formation of smooth surfaces. Therefore, plastic deformation of asperities notably reduced due to the development of the lubricating film between tribopair, which decreases the wear coefficient of H-Al-17Si MMC. The Optical and SEM images (Figs. 18 & 20) show the surface remains smoother at higher applied load (50 N). Moreover, AFM profilometer images also evident the decreased wear scars (R_a=1.35 μm) at 50 N (Fig. 26b) applied load compared to the 30 N load (Ra=3.20 μm) (Fig. 26a).

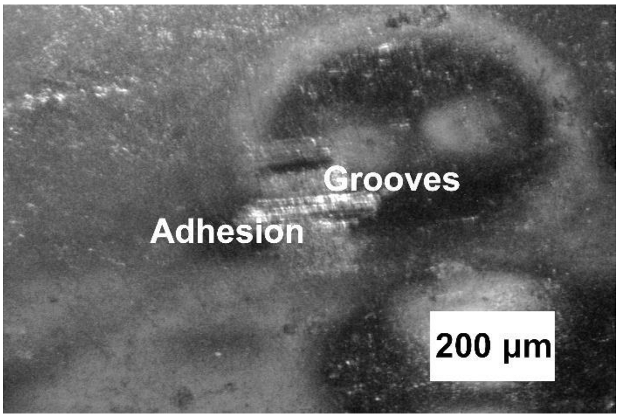

(a)

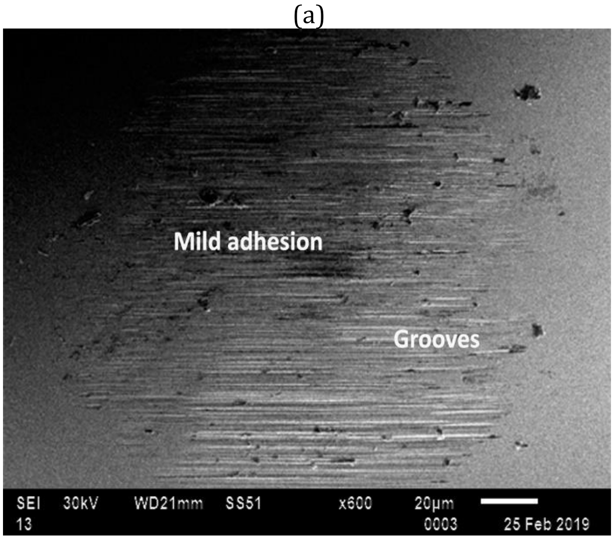

(b)

Fig. 20. (a) Optical micrograph of steel ball at 50 N load under lubricated condition; (b) SEM micrograph of steel ball at 50 N load under lubricated condition.

However, in case coated dry condition, the wear coefficient was reduced significantly as compared to both lubricated (87.9 %) and dry (98.3 %) conditions (Fig. 10). As shown in Figs. 21 and 22, the wear tracks of H-Al-17Si with DLC-Star coating appear smoother and smaller. This is due to the development of a tribo oxidation film, which avoids the mating parts from coming into straight contact and remarkably improves the wear coefficient behavior of the MMC. At the lowest applied load of 10 N, the wear coefficient is nearly negligible due to the higher surface finish of DLC-Star coating. However, with the increasing of applied load (30 N), very thin smaller, and smoother wear scars appear on the surface of the alloy (Figs. 21 and 23) with the increased wear coefficient.

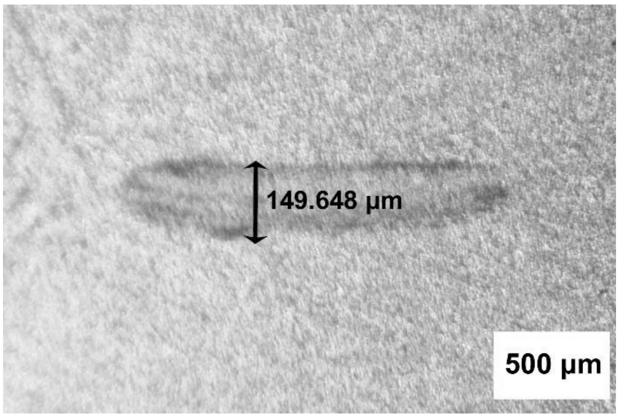

(a)

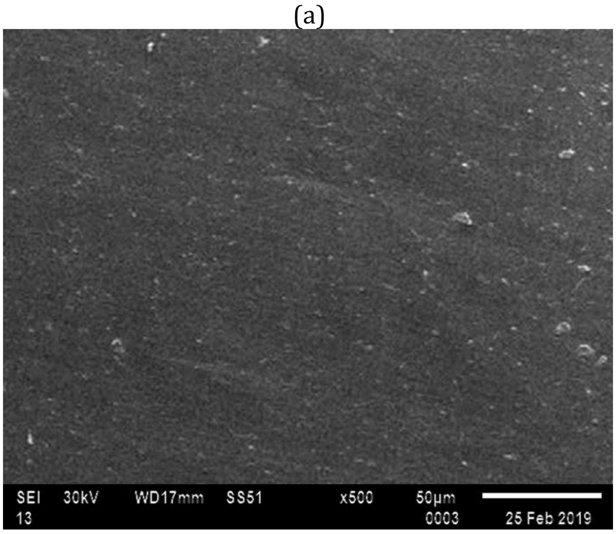

(b)

Fig. 21. (a) Optical micrograph of H-Al-17Si alloy at 30 N load under coated dry condition; (b) SEM micrograph of H-Al-17Si alloy at 30 N load under coated dry condition.

Further, as the load increases to 50 N, the wear coefficient again decreases (Figs. 22 and 24) due to the development of a tribo oxidation film between mating surfaces. The wear scar width in the coated dry condition (Fig. 21) is two times smaller than that of the wear scar (Fig. 18) attained in lubricated condition. Whereas, insignificant wear scars are identified on the AISI52100 ball in case of the coated dry condition (Figs. 23 and 24), which is ascribed to the improved wear resistance of steel ball because of its more hardness (670-770 HV) value as compared to H-Al-17Si MMC disc hardness (165-179.37 HV).

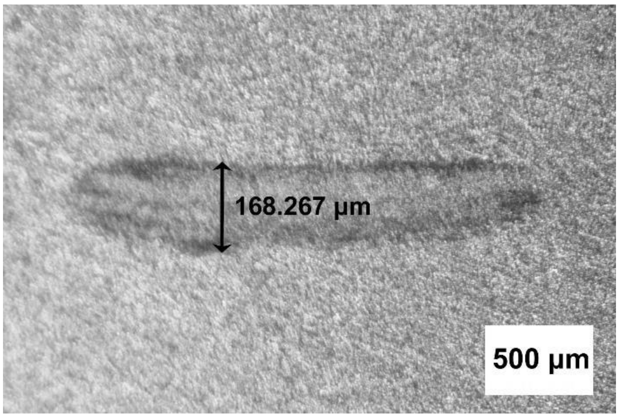

(a)

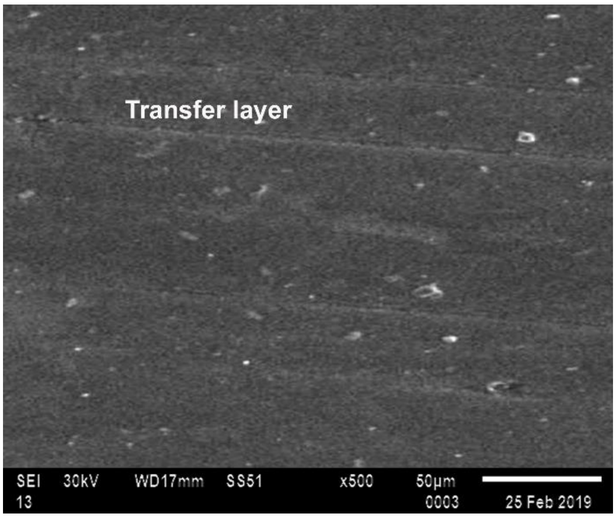

(b)

Fig. 22. (a) Optical micrograph of H-Al-17Si alloy at 50 N load under coated dry condition; (b) SEM micrograph of H-Al-17Si alloy at 50 N load under coated dry condition.

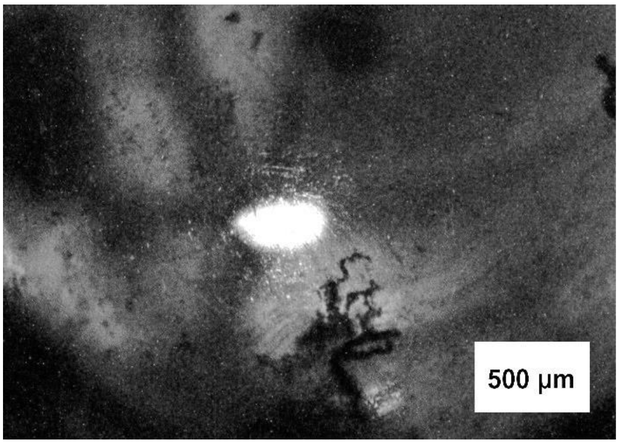

(a)

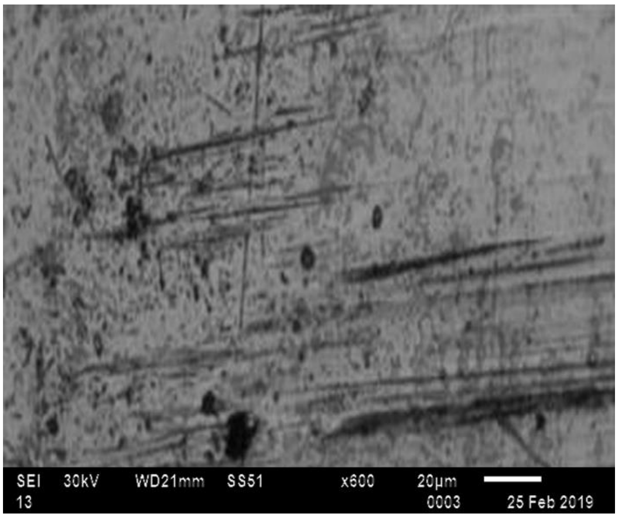

Fig. 23. (a) Optical micrograph of steel ball at 30 N load under coated dry condition; (b) SEM micrograph of steel ball at 30 N load under coated dry condition.

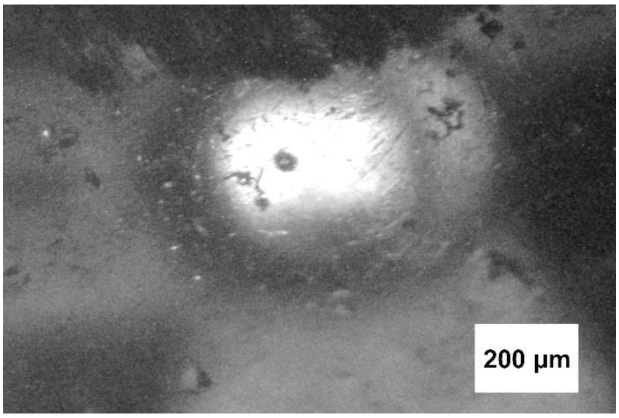

(a)

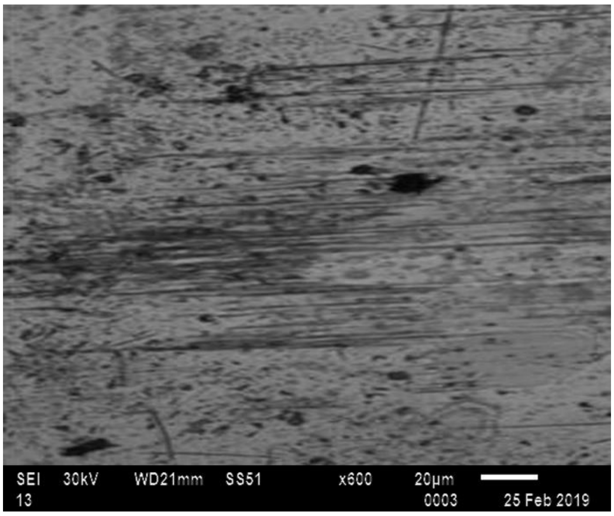

(b)

Fig. 24. (a) Optical micrograph of steel ball at 50 N load under coated dry condition; (b) SEM micrograph of steel ball at 50 N load under coated dry condition.

Further, AFM profilometer images (Figs. 25-27) show that the surface roughness decreases as the applied load increases because of refined hard Si graduals under lubricated, dry, and coated dry conditions. As a result, wear marks of H-Al-17Si MMC disc get softer with increasing applied loads; this action is in accord with the results of the coefficient of wear. At 10 N applied load the maximum roughness value recorded as 10.9 µm (Fig. 25a) with the deep scuffed tracks but when the load increases (30 N) the roughness value increases (19.6 µm) (Fig. 25b) due to adhesion between mating surfaces and when the load further increases (50 N) the roughness value (Fig. 25c) again decreases to 6.8 µm this is due to the formation of oxide layer between tribopair.

Figure 27 represents AFM profilometer images of the wear scars of H-Al-17Si MMC disc undercoated dry condition. As shown in Fig. 27, surface roughness value decreased with increased applied load (10-50 N). The surface roughness value decreased from 0.134 µm (applied load 30 N) to 0.107 (applied load 50 N). The obtained values show that the alloy disc wear scars' surface roughness especially decreases with lubricated and coated dry conditions, while smoother surfaces were obtained with DLC-Star coating. However, the high wear coefficient occurs in the dry state when no protective film presents on the MMC surface (width of the wear mark is 840 µm). It is implicit from these values that DLC-Star coating reduced the wear coefficient of about 60-70 % compared to dry condition. The COF for DLC-Star for H-Al-17Si MMC is the minimum (0.013) throughout the experimental processes as compared to both lubricated and dry environments.

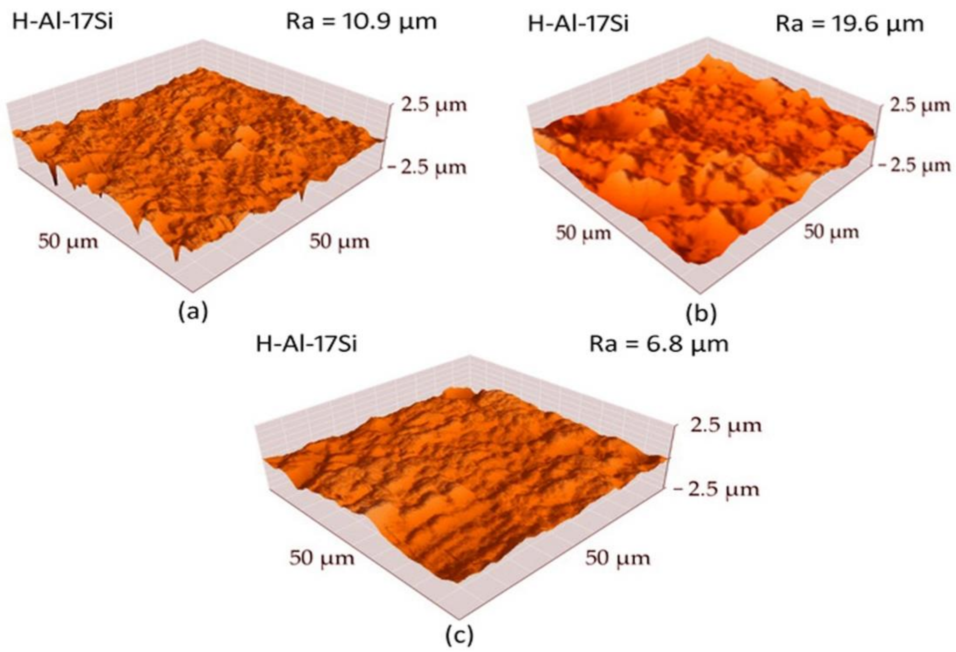

Fig. 25. (a) Surface roughness micrograph of H-Al-17Si alloy at 10 N under dry condition; (b) Surface roughness micrograph of H-Al-17Si alloy at 40 N under dry condition; (c) Surface roughness micrograph of H-Al-17Si alloy at 50 N under dry condition.

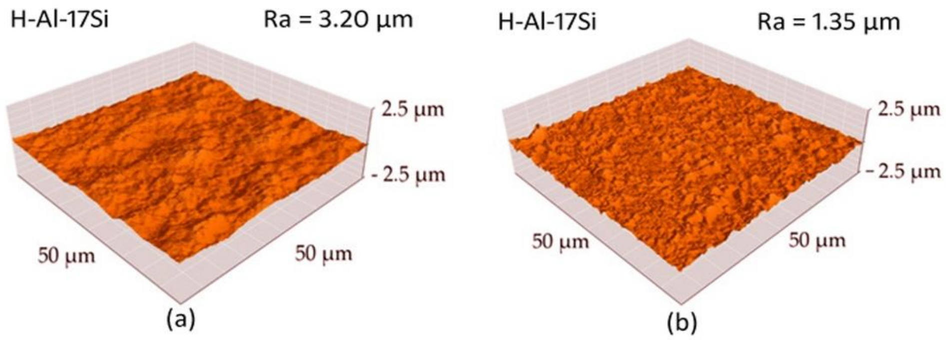

Fig. 26. (a) Surface roughness micrograph of H-Al-17Si alloy at 30 N under lubricated condition (b) Surface roughness micrograph of H-Al-17Si alloy at 50 N under lubricated condition.

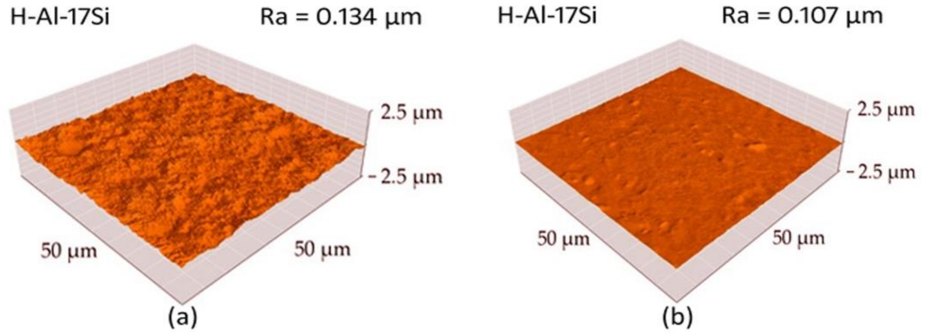

Fig. 27. (a) Surface roughness micrograph of H-Al-17Si alloy at 30 N under coated dry condition; (b) Surface roughness micrograph of H-Al-17Si alloy at 50 N under coated dry condition.

The developments in COF and wear coefficients were mainly attributed to the distribution and size of primary Si granules (Fig. 3a) and the formation of transfer layers on the coated surfaces of AlSi17Cu3.5-4Mg0.6-0.8 alloy (Fig. 22). The anti-wear characteristic of DLC-Star coating for H-Al-17Si disc clearly showed through the optical, SEM, and profilometer micrographs. These results exhibit that DLC-Star coating possesses superior anti-friction and wear characteristics.

From the above results, it is clear that the DLC-Star coating comes up with a new pathway for enhancing the COF and wear characteristics that could be more carry out for many automobile sectors involving linear reciprocating sliding contact surfaces. However, DLC-Star coating is a modified diamond like carbon coating with improved load carrying capacity. An extraordinary hard, sturdy chromium nitride layer gives the required surface hardness and increases the load carrying capacity of the tribologically effective carbon coating. DLC-Star coating has even enhanced friction and wear performance than regular DLC coating. It is therefore used for the highest loaded components in diesel engine parts and injection systems.

4 CONCLUSIONS

In this investigation, we explored the COF and wear characteristics of the DLC-Star coating with H-Al-17Si MMC plate/AISI52100 ball tribopair under different loading (10-50 N) conditions, where PVD/PACVD method is used for the coating of DLC-Star film.

1. The wear and friction coefficients of H-Al-17Si MMC increase with an increase in applied load under dry conditions.
2. Considerable reduction in COF and wear coefficients is adept with SAE15W40 engine oil due to hard Si particles of the MMC act as a solid lubricant in dry as well as lubricated conditions.
3. Substantial effect on reduction of friction and wear coefficients was noticed in the case of H-Al-17Si MMC coated with CrN + a-c:H due to the development of a tribo oxidation film between mating surfaces.

The results reveal that the DLC-Star coating gave a considerable effect on wear and friction coefficients reduction. However, optical, SEM, and AFM roughness profilometer micrographs of mating surfaces evident that the wear and friction coefficients of tribopair reduced significantly from 0.26 to 0.013 and 60-70 %. These solutions exhibit a passivation effect because of DLC-Star coating, which not only helped lower the wear coefficient between mating parts but also supplied easy shearing and therefore resulted in friction improvement. Moreover, these features are essential for automobile engine parts, compressors, soft base materials such as copper or aluminium, and other components exposed to high mechanical loads. Therefore this study gives a new awareness of the relationship between the mating parts and DLC-Star film as good anti-wear and friction coating in industrial or automobile applications.

Acknowledgment

The DLC-Star (CrN + a-c:H) coating on H-Al-17Si was carried out at Oerlikon Balzers Coating India Private Limited with association with Excelanttechnologies, Hyderabad, India, under the coordination of Dinesh Rao .M.A and srinivas@excelanttechnologies.

REFERENCES

[1] P. Kumar, M.F. Wani, *Tribological Characterisation of Graphene Oxide as Lubricant Additive on Hypereutectic Al-25Si/Steel Tribopair,* Tribology Transactions, vol. 61, iss. 2, pp. 335-346, 2018, doi: 10.1080/10402004.2017.1322735

[2] S.D.A. Lawes, M.E. Fitzpatrick, S.V. Hainsworth, *Evaluation of the tribological properties of DLC for engine applications*, Journal of Physics D: Applied Physics, vol. 40, no. 18, pp. 5427– 5437, 2007, doi: 10.1088/0022-3727/40/18/S03

[3] M.D. Sexton, T.E. Fischer, *The Mild Wear of 52100 Steel*, Wear, vol. 96, iss. 1, pp. 17-30, 1987, doi: 10.1016/0043-1648(84)90101-7

[4] H. Czichos, *New Directions for Lubrication, Materials, Wear and Surface Interactions in Tribology in the 80's*, Noyes Publications New Jersey, pp. 891-989, 1989.

[5] M.A. Islam, A.S.M.A. Haseeb, A.S.W. Kurny, *Study of Wear of As-Cast and Heat-Treated Spheroidal Graphite Cast Iron Under Dry Sliding Conditions*, Wear, vol. 188, iss. 1-2, pp. 61-65, 1995, doi: 10.1016/0043-1648(95)06605-5

[6] ASM Handbook, *Friction, Lubrication, and Wear Technology*, ASM International Handbook Committee, vol. 18, no. 785, 1992.

[7] K.M. Jasim, E.S. Dwarakadasa, *Wear in Al-Si Alloys under Dry Sliding Conditions*, Wear, vol. 119, iss. 1, pp. 119-130, 1987, doi: 10.1016/0043-1648(87)90102-5

[8] P.K. Rohatgi, B.C. Pai, *Effect of microstructure and mechanical properties on the seizure resistance of cast aluminium alloy*, Wear, vol. 28, iss. 3, pp. 353-367, 1974, doi: 10.1016/0043-1648(74)90192-6

[9] K.G.B. Kumar, *Influence of Refinement and modification on dry sliding wear behavior of hypereutectic Al-Si cast alloys*, Advanced Materials Research, vol. 685, pp. 112-116, 2013, doi: 10.4028/www.scientific.net/AMR.685.112

[10] N. Nuraliza, S. Syahrullail, M.H. Faizal, *Tribological properties of aluminum lubricated with palm olein at different load using pin-on-disk machine*, Jurnal Tribologi, vol. 9, pp. 45-59, 2016.

[11] C. Lin, S. Wu, S. Lü, P. An, H. Wu, *Effects of high pressure rheo-squeeze casting on Fe-containing intermetallic compounds and mechanical properties of Al-17Si-2Fe-(0, 0.8)V alloys*, Materials Science and Engineering, vol. 713, pp. 105-111, 2018, doi: 10.1016/j.msea.2017.12.050

[12] R.-G. Guan, Z.-Y. Zhao, C.-S. Lee, Q.-S. Zhang, C.-M. Liu, *Effect of wavelike sloping plate rheocasting on microstructures of hypereutectic Al-18 pct Si-5 pct Fe alloys*, Metallurgical and Materials Transactions B, vol. 43, pp. 337-343, 2012, doi: 10.1007/s11663-011-9592-4

[13] D. Pavlyuchkov, S. Balanetskyy, W. Kowalski, M. Surowiec, B. Grushko, *Stable decagonal quasicrystals in the Al-Fe-Cr and Al-Fe-Mn alloy systems*, Journal of Alloys and Compounds, vol. 477, iss. 1-2, pp. L41-L44, 2009, doi: 10.1016/j.jallcom.2008.11.005

[14] Q. Wang, L. Li, R. Zhou, F. Xiao, B. Geng, *Microstructures and wear behavior of the rheo-squeeze casting high silicon aluminium alloys pipe with the gradient structure*, Materials Research Express, vol. 5, no. 10, pp. 106505, 2018, doi: 10.1088/2053-1591/aad9cb

[15] Y. Zhang, J. Jie, Y. Gao, Y. Lu, T. Li, *Effects of ultrasonic treatment on the formation of iron-containing intermetallic compounds in Al-12%Si-2%Fe alloys*, Intermetallics, vol. 42, pp. 120-125, 2013, doi: 10.1016/j.intermet.2013.05.018

[16] Y. Osawa, S. Takamori, T. Kimura, M. Kazumi, K. Hideki, *Morphology of intermetallic compounds in Al-Si-Fe alloy and its control by ultrasonic vibration*, Materials Transactions, vol. 48, iss. 9, pp. 2467-2475, 2007, doi: 10.2320/matertrans.F-MRA2007874

[17] V. Tirth, S. Ray, M.L. Kapoor, *Effect of Squeeze Pressure on Aging and Mechanical Properties of AA2218-5 Wt Pct Al2O3 (TiO2) Composites*, Metallurgical and materials transactions A, vol. 40, pp. 1246-1254, 2009, doi: 10.1007/s11661-009-9815-3

[18] V. Tirth, A. Amir, *Effect of liquid forging pressure on solubility and freezing coefficients of cast aluminum 2124, 2218 and 6063 alloys*, Archives of Metallurgy and Materials, vol. 65, no. 1, pp. 357-366, 2020, doi: 10.24425/amm.2020.131738

[19] A. Edacherian, A. Algahtani, V. Tirth, *Investigations of the Tribological Performance of A390 Alloy Hybrid Aluminum Matrix Composite*, Materials, vol. 11, iss. 12, p. 2524, 2018, doi: 10.3390%2Fma11122524

[20] V. Tirth, A. Algahtani, E.R.I. Mahmoud, *Tribological characterization of stir cast 2218 alloy-5%-alumina-titania hybrid micro composites developed by liquid forging*, Materials Express, vol. 8, no. 6, pp. 475-488, 2018, doi: 10.1166/mex.2018.1464

[21] V. Tirth, *Dry Sliding Wear Behavior of 2218 Al-Alloy-Al2O3(TiO2) Hybrid Composites*, Journal of tribology, vol. 140, iss. 2, pp. 021603-021612, 2018, doi: 10.1115/1.4037697

[22] Khemraj, A.K. Jha, S.N. Ojha, *Tribo-mechanical behavior of complex hypereutectic Al–Si alloy compressed through a converging die at elevated temperatures*, Materials Research Express, vol. 5, no. 7, p. 6509, 2018, doi: 10.1088/2053-1591/aacc94

[23] A. Mahato, S. Xia, T. Perry, A. Sachdev, S.K. Biswas, *Role of Silicon in Resisting Subsurface Plastic Deformation in Tribology of Aluminium–Silicon Alloys*, Tribology International, vol. 43, iss. 1-2, pp. 381-387, 2010, doi: 10.1016/j.triboint.2009.06.020

[24] M. Warmuzek, *Aluminum-Silicon Casting Alloys: An Atlas of Microfractographs*. ASM international, 2004.

[25] J. Clarke, A.D. Sarkar, *Wear Characteristics of As-Cast Binary Aluminum-Silicon Alloys*, Wear, vol. 54, iss. 1, pp. 7-16, 1979, doi: 10.1016/0043-1648(79)90044-9

[26] A.S. Reddy, B.P. Bai, K.S.S. Murthy, S.K. Biswas, *Wear and Seizure of Binary Al- Si Alloys*, Wear, vol. 171, iss. 1-2, pp. 115-127, 1994, doi: 10.1016/0043-1648(94)90354-9

[27] M.S. Kaiser, S.H. Sabbir, M.S. Kabir, M.R. Soummo, M. Al Nur, *Study of Mechanical and Wear Behaviour of Hyper-Eutectic Al-Si Automotive Alloy Through Fe, Ni and Cr Addition*, Materials Research, vol. 21, no. 4, p. e20171096, 2018, doi: 10.1590/1980-5373-MR-2017-1096

[28] C. Bidmeshki, Y. Shajari, V. Abouei, *Tribological Characterization of the Modified Cast Al–Si Eutectic Alloys*, Surface Engineering and Applied Electrochemistry, vol. 55, pp. 183-190, 2019, doi: 10.3103/S1068375519020030

[29] A. Willing, *Lubricants based on renewable resources–an environmentally compatible alternative to mineral oil products*, Chemosphere, vol. 43, iss. 1, pp. 89-98, 2001, doi: 10.1016/S0045-6535(00)00328-3

[30] S.K. Dey, T.A. Perry, A.T. Alpas, *Micromechanisms of Low Load Wear in an Al–18.5% Si Alloy*, Wear, vol. 267, iss. 1-4, pp. 515-524, 2009, doi: 10.1016/j.wear.2008.11.011

[31] P. Kumar, M.F. Wani, *Friction and wear characterization of hypereutectic Al-Si alloy/steel tribopair under dry and lubricated conditions*, Jurnal Tribologi, vol. 15, pp. 21-49, 2017.

[32] P. Kumar, M.F. Wani, *Effect of load on the tribological properties of hypereutectic Al–Si alloy under boundary lubrication conditions*, Material Research Express, vol. 4, iss. 11, p. 6519, 2017, doi: 10.1088/2053-1591/aa98e5

[33] R. Greenberg, G. Halperin, I. Etsion, R. Tenne, *The effect of WS_2 nanoparticles on friction reduction in various lubrication regimes*, Tribology Letters, vol. 17, pp. 179-186, 2004, doi: 10.1023/B:TRIL.0000032443.95697.1d

[34] L. Joly-Pottuz, F. Dassenoy, M. Belin, B. Vacher, J.M. Martin, N. Fleischer, *Ultralow-friction and wear properties of IF-WS_2 under boundary lubrication*, Tribology Letters, vol. 18, pp. 477-485, 2005, doi: 10.1007/s11249-005-3607-8

[35] L. Yadgarov, V. Petrone, R. Rosentsveig, Y. Feldman, R. Tenne, A. Senatore, *Tribological studies of rhenium doped fullerene-like MoS_2 nanoparticles in boundary, mixed and elasto-hydrodynamic lubrication conditions*, Wear, vol. 297, iss. 1-2, pp. 1103-1110, 2013, doi: 10.1016/j.wear.2012.11.084

[36] R. Rosentsveig, A. Gorodnev, N. Feuerstein, H. Friedman, A. Zak, N. Fleischer, J. Tannous, F. Dassenoy, R. Tenne, *Fullerene-like MoS_2 nanoparticles and their tribological behavior*, Tribology Letters, vol. 36, pp. 175-182, 2009, doi: 10.1007/s11249-009-9472-0

[37] Q. Wan, Y. Jin, P. Sun, Y. Ding, *Tribological Behaviour of a Lubricant Oil Containing Boron Nitride Nanoparticles*, Procedia Engineering, vol. 102, pp. 1038-1045, 2015, doi: 10.1016/j.proeng.2015.01.226

[38] M.S. Charoo, M.F. Wani, *Tribological properties of IF-MoS_2 nanoparticles as lubricant additive on cylinder liner and piston ring tribo-pair*, Tribology in Industry, vol. 38, no. 2, pp. 156-162, 2016.

[39] M.S. Charoo, M.F. Wani, *Tribological properties of h-BN nanoparticles as lubricant additive on cylinder liner and piston ring*, Lubrication Science, vol. 29, iss. 4, pp. 241-254, 2016, doi: 10.1002/ls.1366

[40] B.A. Khorramian, G.R. Iyer, S. Kodali, P. Natarajan, R. Tupil, *Review of antiwear additives for crankcase oils*, Wear, vol. 169, iss. 1, pp. 87-95, 1993, doi: 10.1016/0043-1648(93)90394-2

[41] A. Erdemir, M. Switala, R. Wei, P. Wilbur, *A tribological investigation of the graphite-to-diamond-like behavior of amorphous carbon films ion beam deposited on ceramic substrates*, Surface and Coatings Technology, vol. 50, iss. 1, pp. 17-23, 1991, doi: 10.1016/0257-8972(91)90187-2

[42] C. Donnet, A. Grill, *Friction control of diamond-like carbon coatings,* Surface and Coatings Technology, vol. 94-95, pp. 456-462, 1997, doi: 10.1016/S0257-8972(97)00275-2

[43] A. Grill, V. Patel, B.S. Meyerson, *Tribological behavior of diamond-like carbon: effects of preparation conditions and annealing*, Surface

Coating Technology, vol. 49, iss. 1-3, pp. 530-536, 1991, doi: 10.1016/0257-8972(91)90112-A

[44] A. Erdemir, O.L. Eryilmaz, I.B. Nilufer, G.R. Fenske, *Effect of source gas chemistry on tribological performance of diamond-like carbon films*, Diamond and Related Materials, vol. 9, iss. 3-6, pp. 632-637, 2000, doi: 10.1016/S0925-9635(99)00361-1

[45] A. Erdemir, O.L. Eryilmaz, G.R. Fenske, *Synthesis of diamond like carbon films with superlow friction and wear properties*, Journal of Vacuum Science & Technology A, vol. 18, iss. 4, pp. 1987-1992, 2000, doi: 10.1116/1.582459

[46] I. Solomon, A. Sarma, *Tribological and corrosion performance of DLC coating on sintered Al alloy*, Materials Research Express, vol. 6, no. 4, pp. 6412, 2019, doi: 10.1088/2053-1591/aafae2

[47] N. Umehara, T. Kitamura, S. Ito, T. Tokoroyama, M. Murashima, M. Izumida, N. Kawakami, *Effect of Carbonaceous Hard Coatings Overcoat on Friction and Wear Properties for Al Alloy Sliding Bearing in Oil Lubrication*, Advances in Mechanism and Machine Science, IFToMM WC 2019, vol. 73, pp. 3795-3803, 2019, doi: 10.1007/978-3-030-20131-9_376

[48] B. Blanpain, H. Mohrbacher, J.P. Celis, J.R. Roos, *Some aspects of the tribological behavior of diamond and diamondlike carbon coatings under fretting wear conditions*, Diamond Films and Technology, vol. 3, iss. 3, pp. 177-188, 1994.

[49] H. Mohrbacher, B. Blanpain, J.P. Celis, J.R. Roos, *Frictional Behaviour of Diamond-like carbon and diamond coatings in oscillating sliding*, Surface Coating Technology, vol. 62, iss. 1-3, pp. 583-588, 1993, doi: 10.1016/0257-8972(93)90303-6

[50] H. Mohrbacher, J.-P. Celis, *Friction Mechanisms in Hydrogenated Amorphous Carbon Coatings*, Diamond and Related Materials, vol. 4, iss. 11, pp. 1267-1270, 1995, doi: 10.1016/0925-9635(95)00306-1

[51] A. Erdemir, C. Donnet, *Tribology of diamond-like carbon films: Recent progress and future prospects*, Journal of Physics D: Applied Physics, vol. 39, no. 18, pp. R311-R327, 2006, doi: 10.1088/0022-3727/39/18/R01

[52] S. Bhowmick, A.T. Alpas, *The performance of hydrogenated and non-hydrogenated diamond-like carbon tool coatings during the dry drilling of 319 Al*, International Journal of Machine Tools and Manufacture, vol. 48, iss. 7-8, pp. 802-814, 2008, doi: 10.1016/j.ijmachtools.2007.12.006

[53] S. Bhowmick, A.T. Alpas, *Minimum quantity lubrication drilling of aluminium-silicon alloys in water using diamond-like carbon coated drills*, International Journal of Machine Tools and Manufacture, vol. 48, iss. 12-13, pp. 1429-1443, 2008, doi: 10.1016/j.ijmachtools.2008.04.010

[54] S. Bhowmick, M.J. Lukitsch, A.T. Alpas, *Tapping of Al-Si alloys with diamond-like carbon coated tools and minimum quantity lubrication*, Journal of Materials Processing Technology, vol. 210, iss. 15, pp. 2142-2153, 2010, doi: 10.1016/j.jmatprotec.2010.07.032

[55] S. Bhowmick, A.T. Alpas, *The role of diamond-like carbon coated drills on minimum quantity lubrication drilling of magnesium alloys*, Surface and Coatings Technology, vol. 205, iss. 23-24, pp. 5302-5311, 2011, doi: 10.1016/j.surfcoat.2011.05.037

[56] W. Ni, Y.T. Cheng, A.M. Weiner, T.A. Perry, *Tribological behaviour of diamond-like-carbon (DLC) coatings against aluminium alloys at elevated temperatures*, Surface and Coatings Technology, vol. 201, iss. 6, pp. 3229-3234, 2006, doi: 10.1016/j.surfcoat.2006.06.045

[57] A. Erdemir, O.L. Eryilmaz, I.B. Nilufer, G.R. Fenske, *Synthesis of superlow friction carbon films from highly hydrogenated methane plasmas*, Surface Coating Technology, vol. 133-134, pp. 448-454, 2000, doi: 10.1016/S0257-8972(00)00968-3

[58] W.S. Miller, L. Zhuang, J. Bottema, A.J. Wittebrood, P. De Smet, A. Haszler, A. Vieregge, *Recent development in aluminium alloys for the automotive industry*, Materials Science Engineering: A, vol. 280, iss. 1, pp. 37-49, 2000, doi: 10.1016/S0921-5093(99)00653-X

[59] J.R. Davis, *Friction and wear of internal combustion engine parts*, in ASM Handbook, Friction, Lubrication, and Wear Technology, ASM International, Materials Park, OH, vol. 18, no. 10, pp. 553-562, 1992.

[60] E. Konca, Y.-T. Cheng, A.M. Weiner, J.M. Dasch, A.T. Alpas, *Elevated temperature tribological behavior of non-hydrogenated diamond-like carbon coatings against 319 aluminum alloy*, Surface Coating Technology, vol. 200, iss. 12-13, pp. 3996-4005, 2006, doi: 10.1016/j.surfcoat.2005.02.202

[61] E. Konca, Y.-T. Cheng, A.M. Weiner, J.M. Dasch, A. Erdemir, A.T. Alpas, *Transfer of 319 Al alloy to titanium diboride and titanium nitride based (TiAlN, TiCN, TiN) coatings: effects of sliding speed, temperature and environment*, Surface and Coatings Technology, vol. 200, iss. 7, pp. 2260-2270, 2005, doi: 10.1016/j.surfcoat.2004.10.008

[62] K. Saijo, M. Yagi, K. Shibuki, S. Takatsu, *The improvement of the adhesion strength of*

diamond films, Surface and Coatings Technology, vol. 43-44, part 1, pp. 30-40, 1990, doi: 10.1016/0257-8972(90)90057-J

[63] H. Yoshikawa, A. Nishiyama, *CVD diamond coated insert for machining high silicon aluminum alloys*, Diamond Related Materials, vol. 8, iss. 8-9, pp. 1527–1530, 1999, doi: 10.1016/S0925-9635(99)00078-3

[64] S. Bhowmick, A. Banerji, A.T. Alpas, *Tribological behaviour of Al-6.5%, -12%, -18.5% Si alloys during machining using CVD diamond and DLC coated tools*, Surface and Coatings Technology, vol. 284, pp. 353-364, 2015, doi: 10.1016/j.surfcoat.2015.08.073

[65] E. Liu, B. Blanpain, E. Dekempeneer, F. Loffler, J. P. Celis, J. R. Roos, *Mechanical and tribological evaluation of the thermal stability of a-C and a-C:H coatings*, Diamond Films and Technology, vol. 4, iss. 1, pp. 37-49, 1994.

[66] J.K. Walters, D.M. Fox, T.M. Burke, O.D. Weedon, R.J. Newport, W.S. Howells, *The effect of temperature on the structure of amorphous hydrogenated carbon*, The Journal of Chemical Physics, vol. 101, iss. 5, pp. 4288-4300, 1994, doi: 10.1063/1.468427

[67] Y. Bounouh, M.L. Theye, A. Dehbi-Alaoui, A. Matthews, J.P. Stoquert, *Influence of annealing on the hydrogen bonding and the microstructure of diamondlike and polymerlike hydrogenated amorphous carbon films*, Physical Review B, vol. 51, iss. 15, pp. 9597-9605, 1995, doi: 10.1103/PhysRevB.51.9597

[68] C. Wild, P. Koidl, *Proceedings of the E-MRS Meeting*. Strasbourg, Les Editions de Physique, pp. 207-211, 1987.

[69] A. Callegari, D.A. Buchanan, H. Hovel, E. Simonyi, A. Marwick, N.E. Lustig, *Thermal stability and electrical properties of hydrogenated amorphous carbon film*, Applied Physics Letters, vol. 65, iss. 25, pp. 3200-3202, 1994, doi: 10.1063/1.112440

[70] J.E. Hatch, *Aluminium: Properties and Physical Metallurgy*. ASM, Metals Park, OH, pp. 231-32, 1984.

[71] H. Torabian, J.P. Pathak, S.N. Tiwari, *Wear Characteristics of Al-Si Alloys*, Wear, vol. 172, iss. 1, pp. 49-58, 1994, doi: 10.1016/0043-648(94)90298-4

[72] C.M. Chen, C.C. Yang, C.G. Chao, *Dry Sliding Wear Behaviours of Al–25Si–2.5 Cu–1Mg Alloys Prepared by Powder Thixocasting*, Materials Science and Engineering: A, vol. 397, iss. 1-2, pp. 178-189, 2005, doi: 10.1016/j.msea.2005.02.010

[73] N.D. Malleswararao.K, I.N.N. Kumar, *Mechanical Characterization of Rapid Solidified Alsicumg Alloys by New CRSS Casting Method Under T6 Condition*, International Journal of Innovative Technology and Exploring Engineering (IJITEE), vol. 8, iss. 12, pp. 2897-2902, 2019, doi: 10.35940/ijitee.K1577.1081219

[74] N. Saheb, T. Laoui, A.R. Daud, M. Harun, S. Radiman, R. Yahaya, *Influence of Ti Addition on Wear Properties of Al-Si Eutectic Alloys*, Wear, vol. 249, iss. 8, pp. 656-662, 2001, doi: 10.1016/S0043-1648(01)00687-1

Nomenclature

COF	-	Coefficient of friction
DLC	-	Diamond like carbon
RSSC	-	Rheo stir-squeeze casting
MMC	-	Metal matrix composite (alloy)
AFM	-	Atomic force microscope
H-Al-Si	-	Hyper-eutectic aluminum silicon
K_w	-	Wear coefficient, mm^3/Nm
W_v	-	Wear volume, mm^3
S_d	-	Sliding distance, m
R_a	-	Roughness average, μm
F_n	-	Load applied, (N)